Science Advances

AAAS

advances.sciencemag.org/cgi/content/full/2/9/e1600823/DC1

Supplementary Materials for

Cyclic di-GMP mediates a histidine kinase/phosphatase switch by noncovalent domain cross-linking

Badri N. Dubey, Christian Lori, Shogo Ozaki, Geoffrey Fucile, Ivan Plaza-Menacho, Urs Jenal, Tilman Schirmer

Published 16 September 2016, *Sci. Adv.* **2**, e1600823 (2016)
DOI: 10.1126/sciadv.1600823

The PDF file includes:

Other Supplementary Material for this manuscript includes the following:
(available at advances.sciencemag.org/cgi/content/full/2/9/e1600823/DC1)

- database S1 (Microsoft Excel format). Bacterial strains used in this study.
- database S2 (Microsoft Excel format). Plasmids used in this study.
- database S3 (Microsoft Excel format). Oligonucleotides used in this study.

table S1. Data collection and refinement statics.

	CckA_CA/AMPPNP/ c-di-GMP/Mg^{2+}	CckA_DHp-CA/ADP/Mg^{2+}
Data collection		
Synchrotron source	SLS, PXIII	SLS, PXI
Space group	P 2_1 2_1 2_1	P 6_3 2 2
a, b, c (Å)	56.3, 62.1, 103.9	164.9, 164.9, 48.0
α, β, γ (^{0})	90, 90, 90	90, 90,120
Resolution (Å)	30-1.9 (2.0-1.9)*	30-3.0 (3.1-3.0)
Unique reflections	29150 (4197)	7413 (575)
Completeness	99.2 (99.3)	91.4 (51.2)
I/σ(I)	13.8 (5.9)	15.0 (1.7)
Redundancy	6.4 (6.5)	11.3 (1.6)
R_{merge} (%)	8.8 (30.0)	10.3 (32.7)
R_{pim} (%)	3.8 (16.3)	3.1 (28.6)
CC (1/2) %	99.8 (91.9)	99.9 (77.4)
Refinement		
R_{work}/R_{free} (%)	18.7/22.5	21.1/27.8
rmsd		
Bond length (Å)	0.009	0.011
Bond angles (°)	1.62	1.65
Molecules/asymmetric unit	2	1
No. of atoms		
Protein	2735	1869
Ligand	110	28
Metals	2	1
Water	428	1
Average B-factor ($Å^2$)	17.6	90
Protein	16.9	90.3
Nucleotides	8	74.1
Metals	10.1	63.5
Water	24.6	61.3
Ramachandran statistics (%)		
Favored regions	97.1	87.9
Allowed regions	2.6	9.2
Disallowed regions	0.3	2.9
PDB codes	5IDM	5IDJ

* The values recorded in parentheses are those for the highest resolution shell

table S2. Thermodynamic parameters of CckA-ligand interactions as measured by ITC.

(a) ADP binding*								
CckA construct	c_{cell} (μM)	$c_{syringe}$ (μM)	- c-di-GMP			+ 100 μM c-di-GMP†		
			K_d (mM)	ΔH (kcal/mol)	-TΔS (kcal/mol)	K_d (μM)	ΔH (kcal/mol)	-TΔS (kcal/mol)
CA	76	5000	1	-4.8	0.8	Nd		
ΔTM	50	5000	0.53	-1.6	-2.9	‡	~ 0.3	
ΔTM G318A	50	5000	0.20	-4.9	-4.5	Nd		
ΔTM R374A	50	5000	0.36	-2.2	-2.5	Nd		

(b) AMPPNP binding								
CckA construct	c_{cell} (μM)	$c_{syringe}$ (μM)	- c-di-GMP			+ 100 μM c-di-GMP		
			K_d (μM)	ΔH (kcal/mol)	-TΔS (kcal/mol)	K_d (μM)	ΔH (kcal/mol)	-TΔS (kcal/mol)
CA	20	800	12	-1.9	-4.5	43	-2.4	-3.3
ΔTM	20	800	9.7	-1.4	-5.2	57	-2.5	-3
ΔTM G318A	40	1000	25.0	-4.9	-1.2	Nd		
ΔTM R374A	40	600	no significant binding			Nd		

(c) c-di-GMP binding								
CckA construct	c_{cell} (μM)	$c_{syringe}$ (μM)	+ 5 mM ADP			+ 5 mM AMPPNP		
			K_d (μM)	ΔH (kcal/mol)	-TΔS (kcal/mol)	K_d (μM)	ΔH (kcal/mol)	-TΔS (kcal/mol)
CA	20/44	400/600	22	2.2	-8.3	25	2	-8
DHp-CA	45/40	700/800	34	0.9	-6.7	33	1	-6.9
ΔTM	20	400/800	1.4	4.9	-12.5	No significant binding		
ΔTM G318A	50	800	34	0.9	-6.7	Weak binding		
ΔTM R374A	50	800	25	1	-7	48	0.7	-6.3

Raw data and fits to the data are shown in fig. S4. The data were measured at 25°C (ADP) or 12°C (AMPPNP, c-di-GMP). The cell volume was 1.4 ml, the syringe volume 300 μL.

* Heat of ADP dilution has been subtracted from the data.

† Note that at the employed concentration, the protein is not saturated with c-di-GMP at the start of titration. Thus, upon titration, a contribution to the generated heat by c-di-GMP binding or unbinding should be considered. Furthermore, the problem is compounded by the distinct sign of the two ΔH contributions (endo- and exothermic binding of c-di-GMP and mono-nucleotide, respectively). Therefore, the given values have to be considered as effective parameters only.

‡ No reliable fit due to very low signal.

table S3. Kinetic parameters of HK/phosphatase CckA_ΔTM.

Rate and dissociation constants	Value
auto-phosphorylation rate (k_1)	$2.6 \cdot 10^{-3}$ s^{-1}
auto-dephosphorylation rate (k_2)	$2.1 \cdot 10^{-2}$ s^{-1}
ATP binding off-rate (k_{r1})	0.46 s^{-1}
ADP binding off-rate (k_{r2})	$7.0 \cdot 10^{-3}$ s^{-1}
CckA/ATP affinity (K_{d1})	9.7 µM *
CckA/ADP affinity, - c-di-GMP (K_{d2})	0.53 mM *
CckA/ADP affinity, + c-di-GMP ($K_{d2'}$)	0.3 µM

Parameters were obtained from the fit of the kinetic model (Fig. 7) to the data shown in Fig. 5B. In addition, a scale-factor was refined that relates autoradiograph readings to the concentration of CckA-ΔTM~P.

* not refined, set to apparent K_d obtained by ITC for ADP or AMPPNP (table S2).

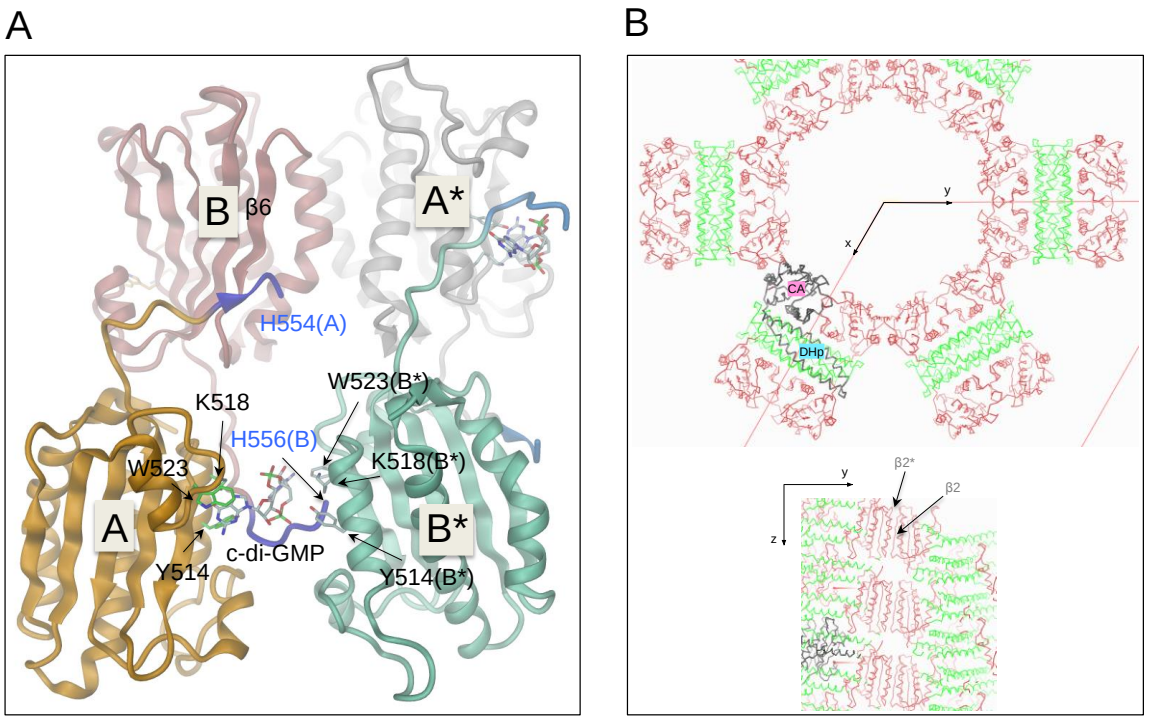

fig. S1. CckA crystal packings. (A) Crystal packing of CckA_CA with two molecules in asymmetric unit (A, B); also shown are two symmetry related molecules (A*, B*). The C-terminal His(6)-tails are colored in blue. C-di-GMP is bound to the primary site of molecule A (orange), whereas the primary binding site of B* (green) is blocked by the His-tail of the symmetry related B chain. The His-tail of A interacts laterally with β6 at the edge of the β-sheet edge of B. **(B)** Two orthogonal views of the CckA_DHp-CA crystal packing. The crystal of space-group $P6_322$ is formed by β-sheet edge-to-edge association (β2 / β2*) of CA domains (red) across crystallographic dyads. In combination with the crystallographic 6_3 screw axis, nano-tubes with a diameter of 45 Å are formed in the z-direction. The nano-tubes are held together by DHp domains (green) that form crystallographic dimers.

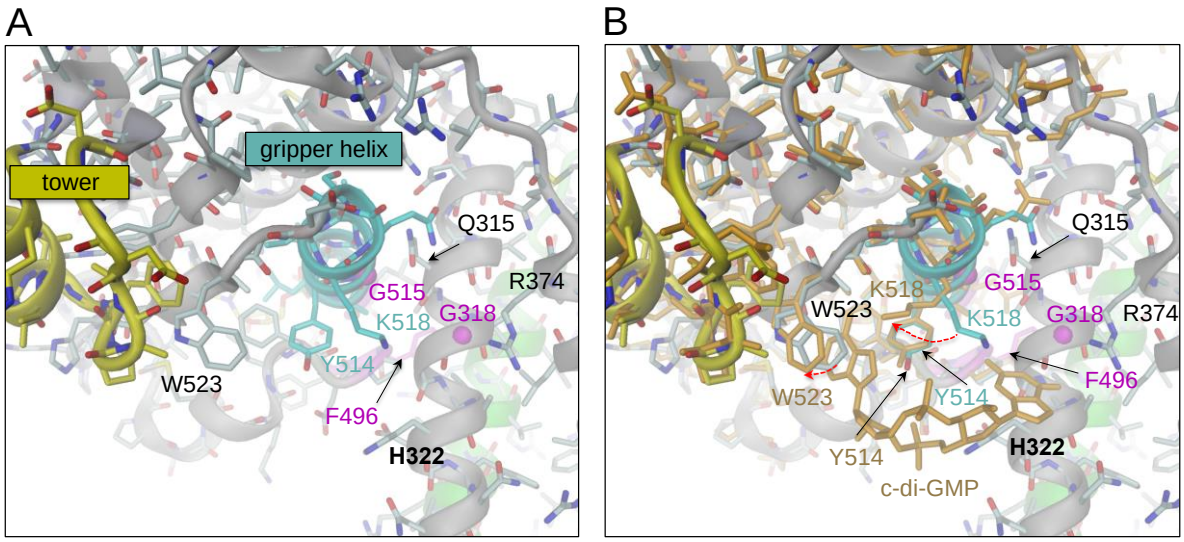

fig. S2. Detailed view of domain interface of CckA_DHp-CA and comparison with c-di-GMP–bound CckA_CA. Viewing direction same as in Fig. 2. The "gripper" helix (residues 509 - 520) and the tower (456 - 471) are shown in cyan and yellow, respectively. The Cα atoms of Gly318 and Gly515 are shown as magenta spheres. **(A)** CckA_DHp-CA crystal structure. **(B)** Same as (**A**), but showing, in addition, the crystal structure of CckA_CA with bound c-di-GMP (all atoms, orange) superimposed. The two major local changes induced by c-di-GMP binding (K518, W523) are indicated by red broken arrows.

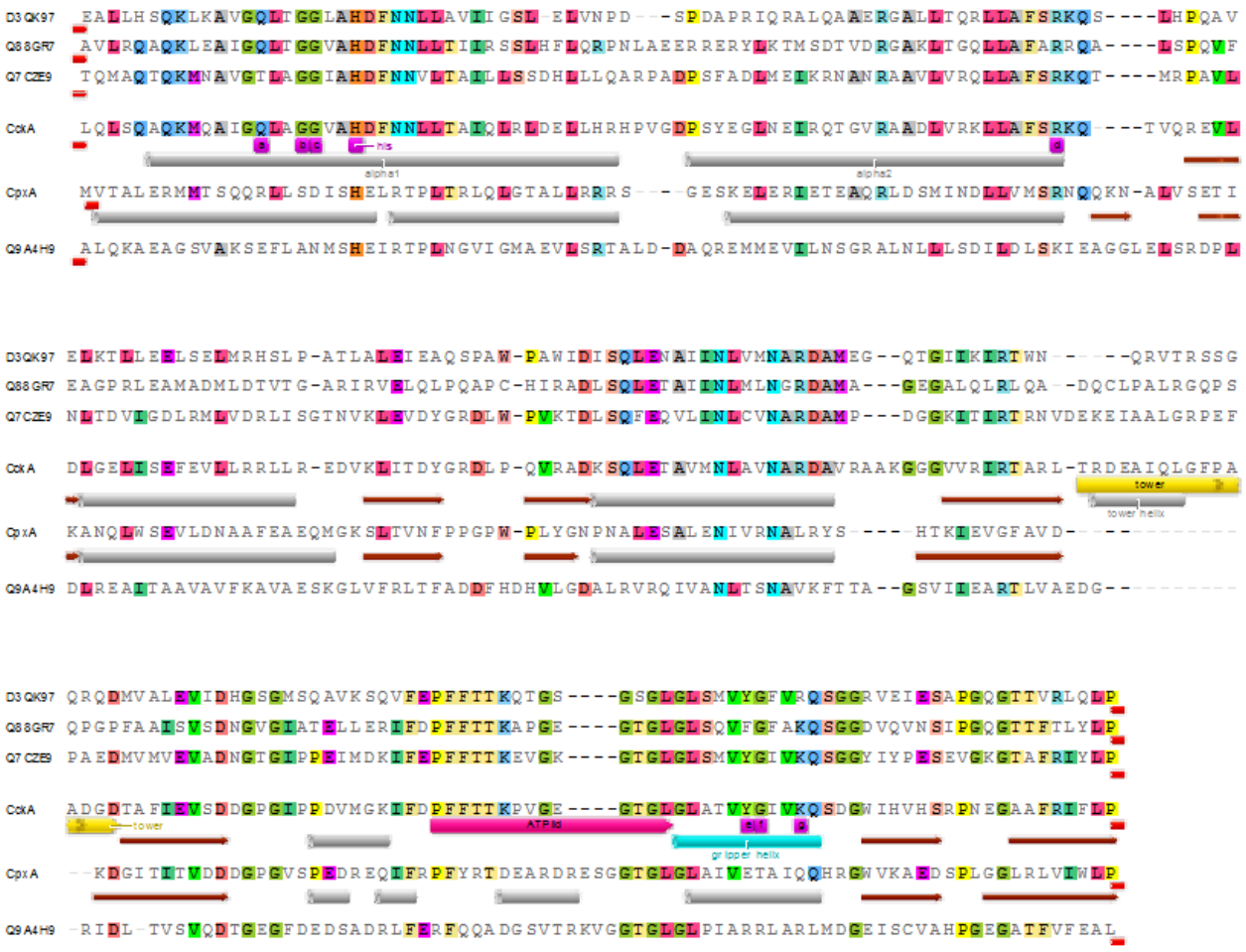

fig. S3. Sequence alignment between CckA orthologs and paralogs. CckA orthologs from UPEC *E. coli* (UNIPROT D3QK97), *Pseudomonas putida* (Q88GR7), *Agrobacterium tumefaciens* (Q7CZE9), and CckA from *Caulobacter crescentus* (H7C7G9) are shown at the top. Paralogs CpxA from *E. coli* (P0AE82) and Q9A4H9 from *C. crescentus* are shown at the bottom. Residue numbers refer to CckA. The sequence alignment between CckA and CpxA conforms to the alignment between the crystal structures and secondary structure elements are indicated. Important CckA residues are annotated: **a**, Q315; **b-c**, G318, G319; **d**, R374; **e**, Y514; **f**, G515; **g**, K318. All of these residues are specifically conserved in the orthologous group.

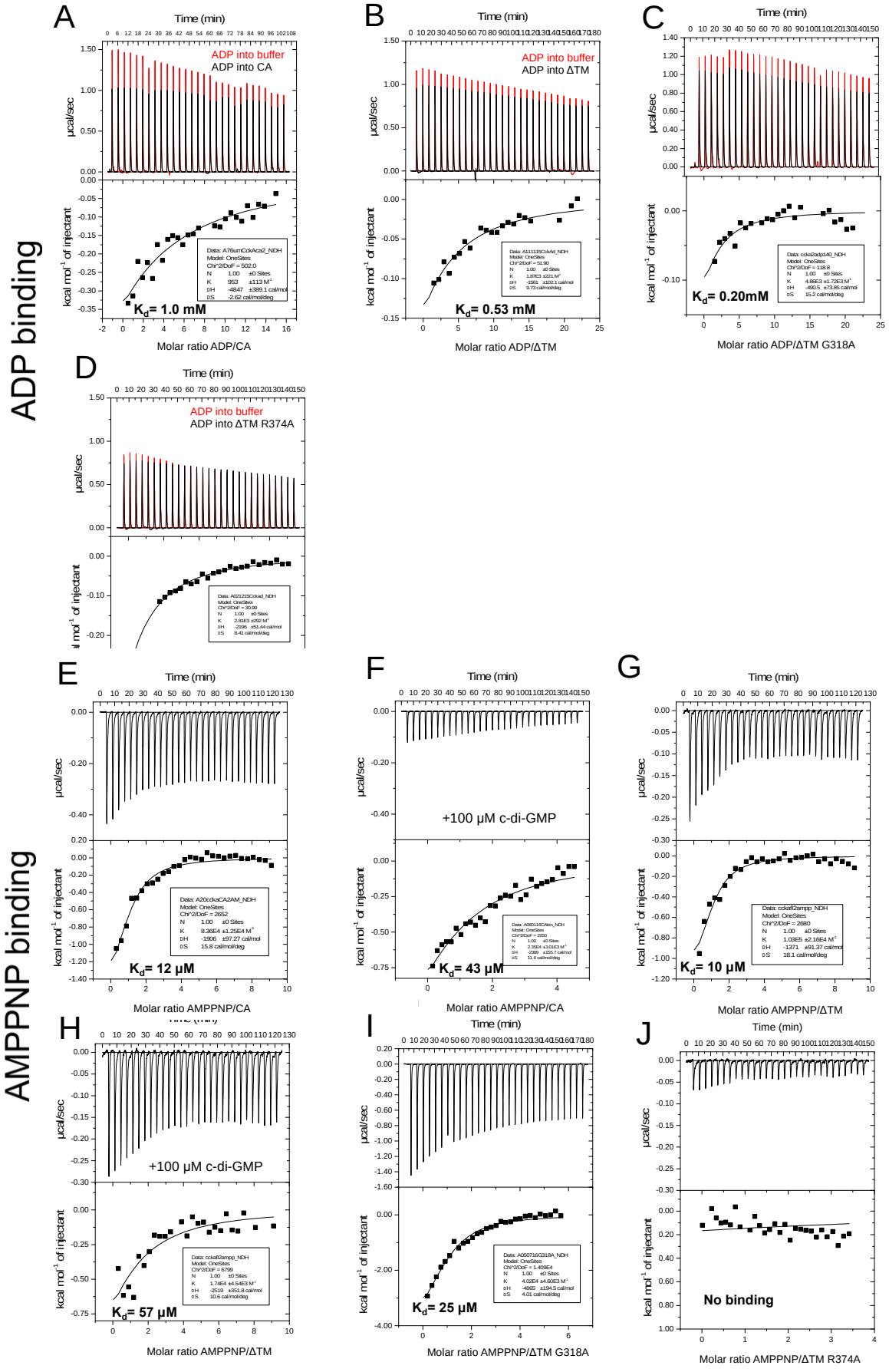
ADP binding
AMPPNP binding
A
Time (min)
ADP into buffer
ADP into CA
µcal/sec
kcal mol-1 of injectant
Kd= 1.0 mM
Molar ratio ADP/CA
B
Time (min)
ADP into buffer
ADP into ΔTM
µcal/sec
kcal mol-1 of injectant
Kd= 0.53 mM
Molar ratio ADP/ΔTM
C
Time (min)
µcal/sec
kcal mol-1 of injectant
Kd= 0.20mM
Molar ratio ADP/ΔTM G318A
D
Time (min)
ADP into buffer
ADP into ΔTM R374A
µcal/sec
E
Time (min)
µcal/sec
kcal mol-1 of injectant
Kd= 12 µM
Molar ratio AMPPNP/CA
F
Time (min)
+100 µM c-di-GMP
µcal/sec
kcal mol-1 of injectant
Kd= 43 µM
Molar ratio AMPPNP/CA
G
Time (min)
µcal/sec
kcal mol-1 of injectant
Kd= 10 µM
Molar ratio AMPPNP/ΔTM
H
+100 µM c-di-GMP
µcal/sec
kcal mol-1 of injectant
Kd= 57 µM
Molar ratio AMPPNP/ΔTM
I
Time (min)
µcal/sec
kcal mol-1 of injectant
Kd= 25 µM
Molar ratio AMPPNP/ΔTM G318A
J
Time (min)
µcal/sec
kcal mol-1 of injectant
No binding
Molar ratio AMPPNP/ΔTM R374A

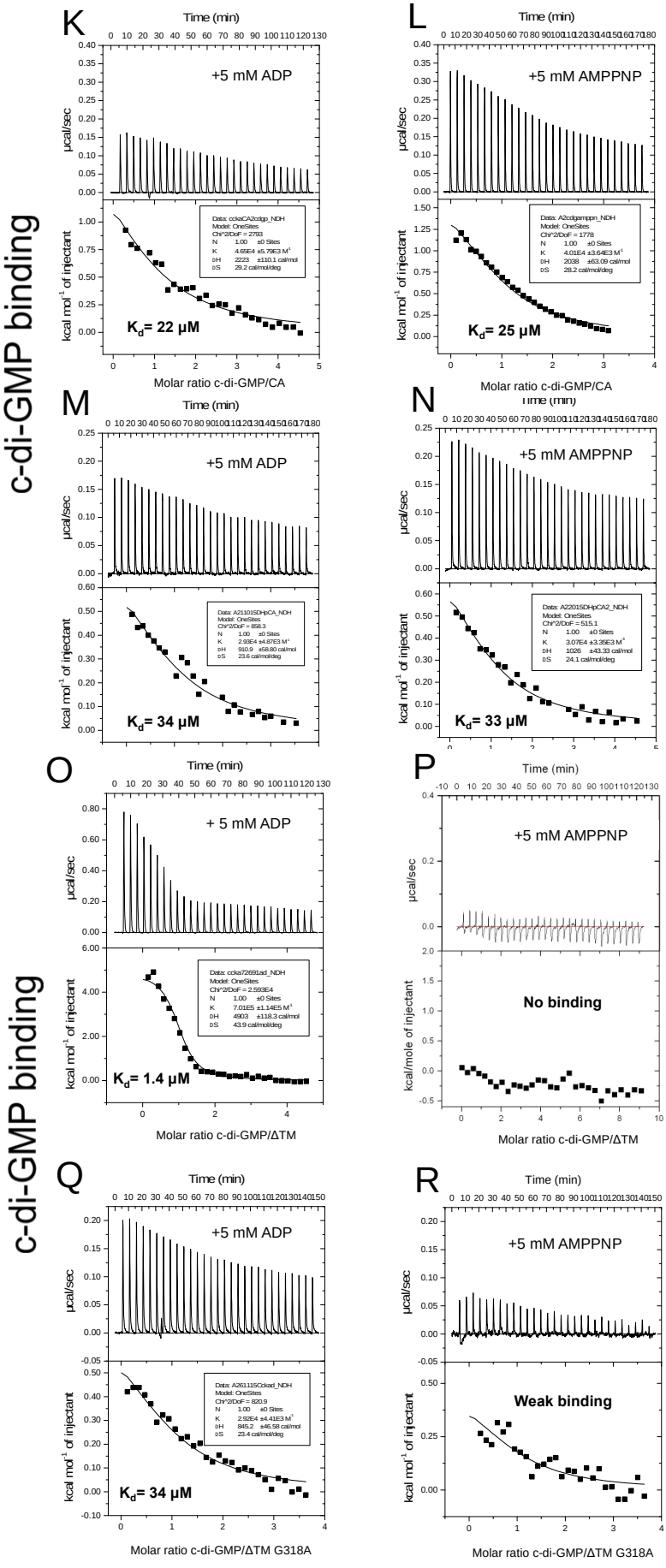
c-di-GMP binding
K
Time (min)
+5 mM ADP
µcal/sec
kcal mol-1 of injectant
Kd= 22 µM
Molar ratio c-di-GMP/CA
L
Time (min)
+5 mM AMPPNP
µcal/sec
kcal mol-1 of injectant
Kd= 25 µM
Molar ratio c-di-GMP/CA
M
Time (min)
+5 mM ADP
µcal/sec
kcal mol-1 of injectant
Kd= 34 µM
N
+5 mM AMPPNP
µcal/sec
kcal mol-1 of injectant
Kd= 33 µM
c-di-GMP binding
O
Time (min)
+ 5 mM ADP
µcal/sec
kcal mol-1 of injectant
Kd= 1.4 µM
Molar ratio c-di-GMP/ΔTM
P
Time (min)
+5 mM AMPPNP
µcal/sec
kcal/mole of injectant
No binding
Molar ratio c-di-GMP/ΔTM
Q
Time (min)
+5 mM ADP
µcal/sec
kcal mol-1 of injectant
Kd= 34 µM
Molar ratio c-di-GMP/ΔTM G318A
R
Time (min)
+5 mM AMPPNP
µcal/sec
kcal mol-1 of injectant
Weak binding
Molar ratio c-di-GMP/ΔTM G318A

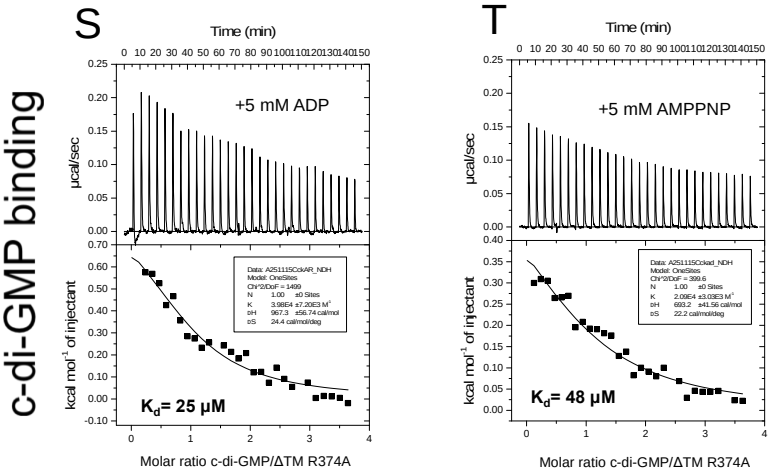

fig. S4. ITC ligand-binding profiles for several CckA. (A-D), ADP binding. Data were evaluated taking into account the large heat of dilution (red trace) due to the high amount of ADP in each injection. **(E-J)**, AMPPNP binding in absence and presence of c-di-GMP. **(K-T)**, c-di-GMP binding in presence of ADP or AMPPNP. Experimental conditions and the resulting thermodynamic parameters are given in table S2.

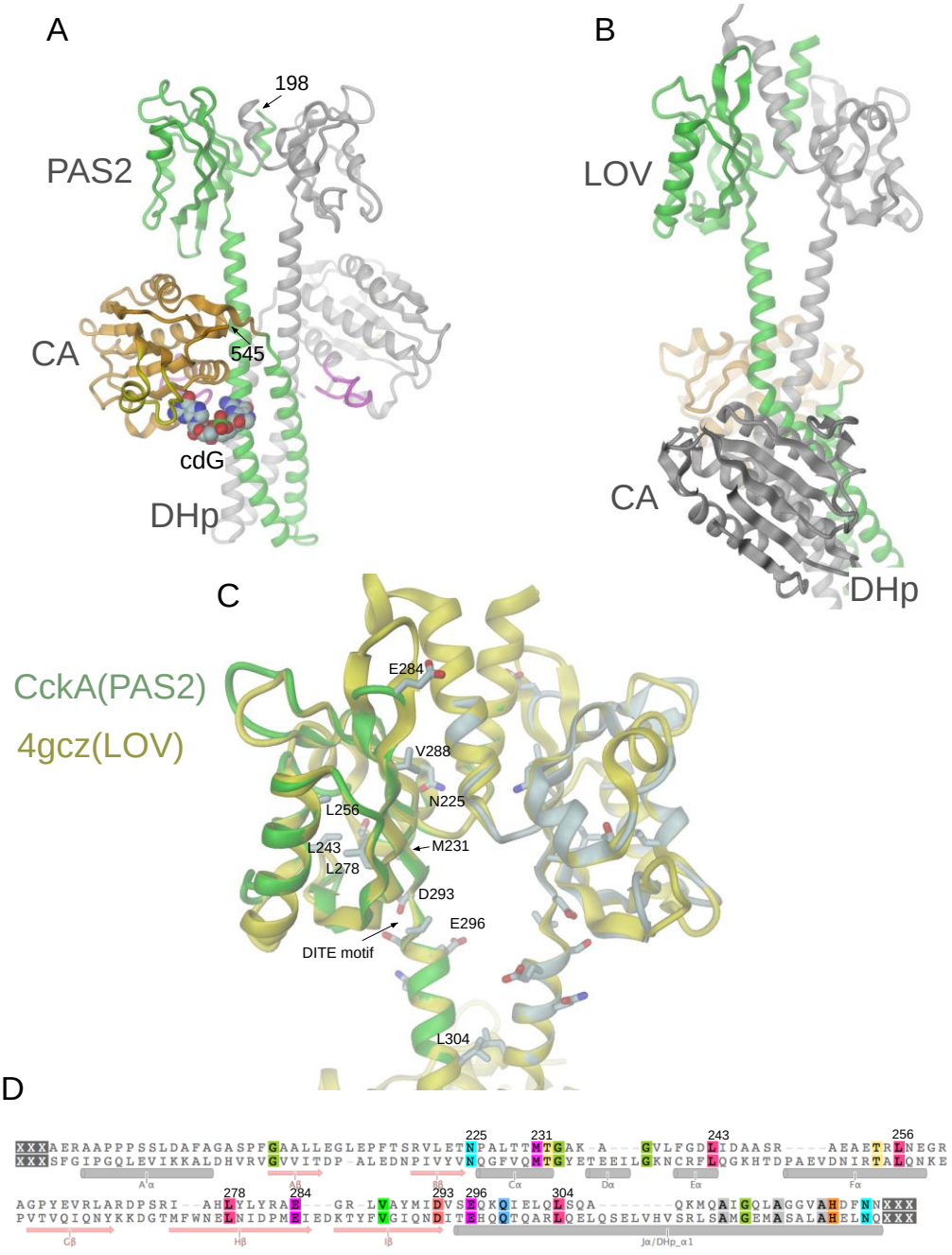

fig. S5. Structure prediction for PAS2 domain of CckA. (A) CckA_DHp-CA structure with joined homology model for the N-terminal PAS2 dimer. The PAS2 homology model was obtained based on PDB entry 4gcz (structure of an engineered LOV-DHp-CA construct based on the LOV domain of YtvA and the DHp-CA domains of FixL (*8*)) using SwissModel (*45*) (qmean4 = -3.28). **(B)** YtvA/FixL template structure (PDB code 4gcz). Orientation such that the N-terminal LOV dimer is in same orientation as the PAS2 dimer in (**A**). **(C)** Sequence alignment of CckA_PAS2-DHp with YtvA(LOV)-FixL(DHp) as obtained by SwissModel and used for homology modeling. Note that the domain linker is shorter by 7 residues in CckA, which is compatible with a coiled-coil dimer shortened by two turns.

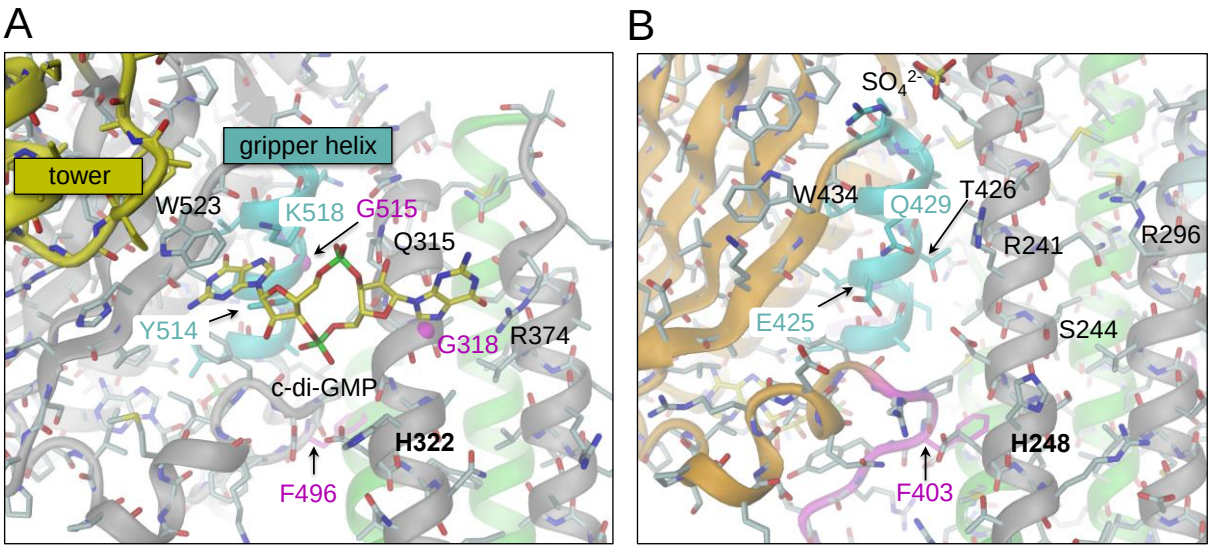

fig. S6. Proposed model of noncovalent c-di-GMP–mediated cross-linking of the CA with the DHp domain of CckA. (A) CckA model obtained by superposition of its individual DHp helices and its CA domain onto the CpxA/ADP structure (*17*). The distal part of the c-di-GMP ligand (right) has been remodeled in extended conformation as observed when bound to the YahA EAL domain (*46*). The side-chain conformation of Arg374 has been adjusted to allow interaction with the c-di-GMP ligand. The Cα atoms of Gly318 and Gly515 are shown as magenta spheres. **(B)** Structure of CpxA/ADP in same view, for comparison. Phe403 (shown in magenta) is engaged in the CA–DHp interface, but all residues crucial for c-di-GMP binding in CckA are not conserved.

A

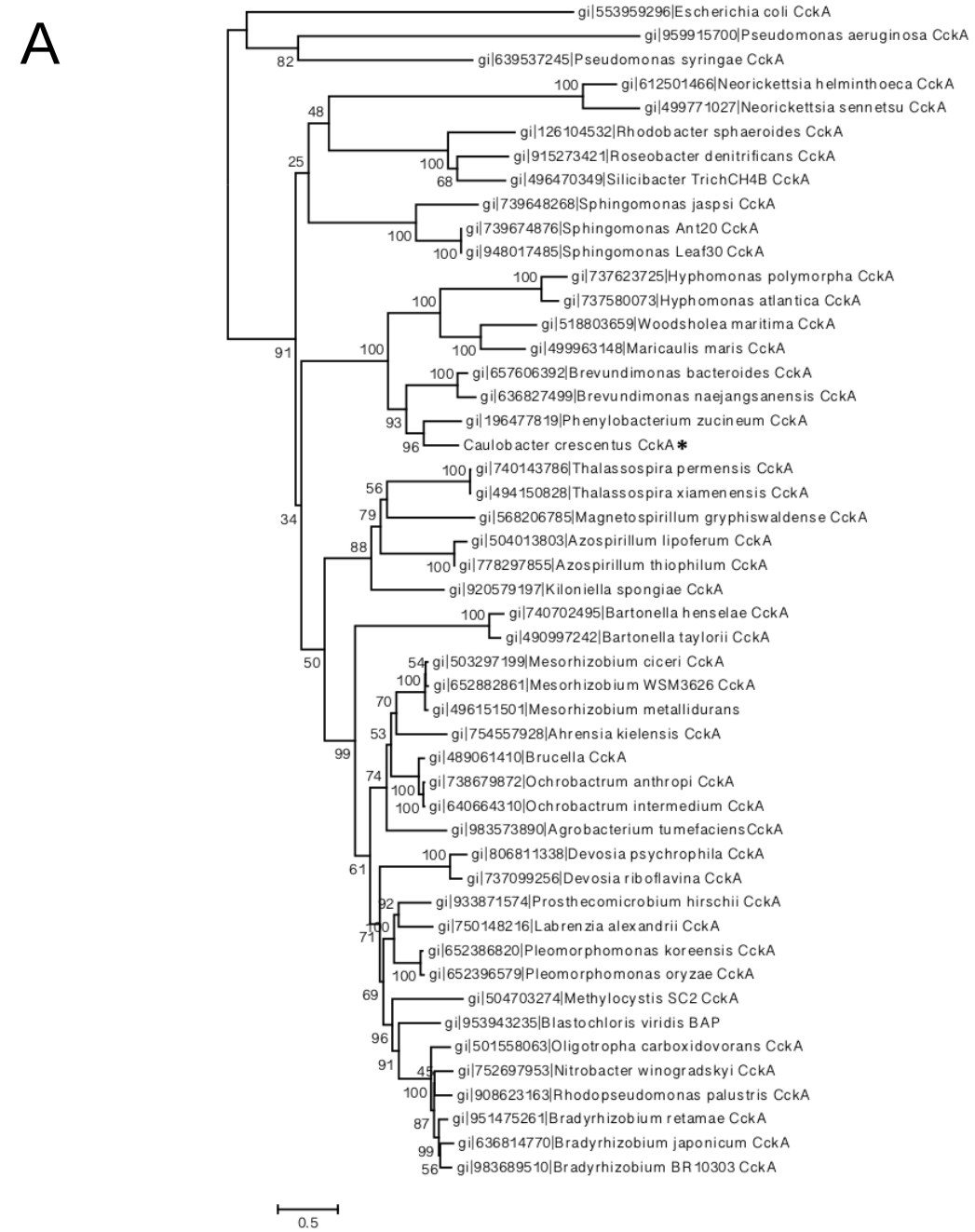
gi|553959296|Escherichia coli CckA
gi|959915700|Pseudomonas aeruginosa CckA
gi|639537245|Pseudomonas syringae CckA
gi|612501466|Neorickettsia helminthoeca CckA
gi|499771027|Neorickettsia sennetsu CckA
gi|126104532|Rhodobacter sphaeroides CckA
gi|915273421|Roseobacter denitrificans CckA
gi|496470349|Silicibacter TrichCH4B CckA
gi|739648268|Sphingomonas jaspsi CckA
gi|739674876|Sphingomonas Ant20 CckA
gi|948017485|Sphingomonas Leaf30 CckA
gi|737623725|Hyphomonas polymorpha CckA
gi|737580073|Hyphomonas atlantica CckA
gi|518803659|Woodsholea maritima CckA
gi|499963148|Maricaulis maris CckA
gi|657606392|Brevundimonas bacteroides CckA
gi|636827499|Brevundimonas naejangsanensis CckA
gi|196477819|Phenylobacterium zucineum CckA
Caulobacter crescentus CckA*
gi|740143786|Thalassospira permensis CckA
gi|494150828|Thalassospira xiamenensis CckA
gi|568206785|Magnetospirillum gryphiswaldense CckA
gi|504013803|Azospirillum lipoferum CckA
gi|778297855|Azospirillum thiophilum CckA
gi|920579197|Kiloniella spongiae CckA
gi|740702495|Bartonella henselae CckA
gi|490997242|Bartonella taylorii CckA
gi|503297199|Mesorhizobium ciceri CckA
gi|652882861|Mesorhizobium WSM3626 CckA
gi|496151501|Mesorhizobium metallidurans
gi|754557928|Ahrensia kielensis CckA
gi|489061410|Brucella CckA
gi|738679872|Ochrobactrum anthropi CckA
gi|640664310|Ochrobactrum intermedium CckA
gi|983573890|Agrobacterium tumefaciensCckA
gi|806811338|Devosia psychrophila CckA
gi|737099256|Devosia riboflavina CckA
gi|933871574|Prosthecomicrobium hirschii CckA
gi|750148216|Labrenzia alexandrii CckA
gi|652386820|Pleomorphomonas koreensis CckA
gi|652396579|Pleomorphomonas oryzae CckA
gi|504703274|Methylocystis SC2 CckA
gi|953943235|Blastochloris viridis BAP
gi|501558063|Oligotropha carboxidovorans CckA
gi|752697953|Nitrobacter winogradskyi CckA
gi|908623163|Rhodopseudomonas palustris CckA
gi|951475261|Bradyrhizobium retamae CckA
gi|636814770|Bradyrhizobium japonicum CckA
gi|983689510|Bradyrhizobium BR10303 CckA
0.5

B

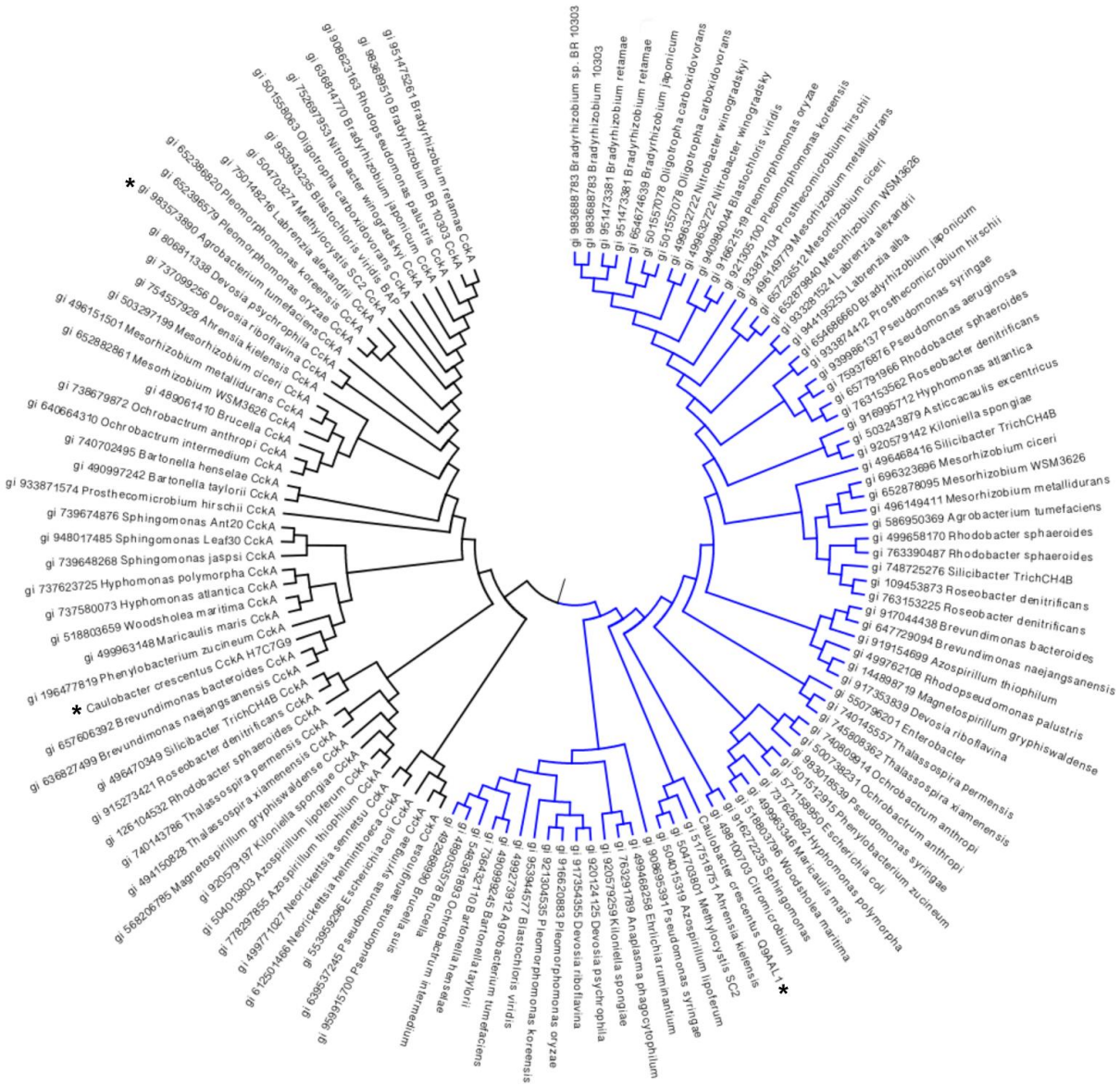
gi 983688783 Bradyrhizobium sp. BR 10303
gi 983688783 Bradyrhizobium 10303
gi 951473381 Bradyrhizobium retamae
gi 951473381 Bradyrhizobium retamae
gi 654674639 Bradyrhizobium retamae
gi 501557078 Oligotropha carboxidovorans
gi 501557078 Oligotropha japonicum
gi 499632722 Nitrobacter winogradskyi
gi 940984044 Blastochloris viridis
gi 916621519 Pleomorphomonas oryzae
gi 923095100 Pleomorphomonas koreensis
gi 933874104 Prosthecomicrobium hirschii
gi 496149779 Mesorhizobium metallidurans
gi 652736512 Mesorhizobium ciceri
gi 652878940 Mesorhizobium WSM3626
gi 933281524 Labrenzia alexandrii
gi 944195253 Labrenzia alba
gi 654686660 Bradyrhizobium japonicum
gi 933874412 Prosthecomicrobium hirschii
gi 939986137 Pseudomonas syringae
gi 759376876 Pseudomonas aeruginosa
gi 657791966 Rhodobacter sphaeroides
gi 763153562 Rhodobacter denitrificans
gi 916995712 Roseobacter atlantica
gi 503243879 Hyphomonas excentricus
gi 920579142 Asticcacaulis sp. BAP
gi 496468416 Kiloniella spongiae
gi 696323696 Silicibacter TrichCH4B
gi 652878095 Mesorhizobium ciceri
gi 496149411 Mesorhizobium WSM3626
gi 586950369 Mesorhizobium metallidurans
gi 499658170 Agrobacterium tumefaciens
gi 763390487 Rhodobacter sphaeroides
gi 748725276 Rhodobacter sphaeroides
gi 109453873 Silicibacter TrichCH4B
gi 763153225 Roseobacter denitrificans
gi 917044438 Roseobacter denitrificans
gi 647729094 Brevundimonas bacteroides
gi 919154699 Brevundimonas naejangsanensis
gi 499762108 Azospirillum thiophilum
gi 14489819 Rhodopseudomonas palustris
gi 917353839 Magnetospirillum gryphiswaldense
gi 550796201 Devosia riboflavina
gi 740145557 Enterobacter
gi 745809362 Thalassospira permensis
gi 740809814 Thalassospira xiamenensis
gi 500738231 Ochrobactrum anthropi
gi 501512915 Pseudomonas syringae
gi 571158950 Phenylobacterium zucineum
gi 737626692 Escherichia coli
gi 499983798 Hyphomonas polymorpha
gi 516803346 Woodsholea maritima
gi 916272235 Maricaulis maris
gi 498100103 Sphingomonas
gi 517518751 Citromicrobium
gi 504703801 Methylocystis SC2
gi 504015319 Ahrensia kielensis Q9AAL1
gi 908695391 Azospirillum lipoferum
gi 499468258 Pseudomonas syringae
gi 763291789 Enhrichia ruminantium
gi 920579259 Anaplasma phagocytophilum
gi 920124125 Kiloniella spongiae
gi 917354355 Devosia psychrophila
gi 916620883 Devosia riboflavina
gi 921304535 Pleomorphomonas oryzae
gi 499273912 Pleomorphomonas koreensis
gi 953944577 Blastochloris viridis
gi 480998245 Agrobacterium tumefaciens
gi 736422110 Bartonella taylorii
gi 548961953 Bartonella henselae
gi 489288990 Ochrobactrum intermedium
gi 489053578 Brucella sp.
gi 553952986 Escherichia coli CckA
gi 639537245 Pseudomonas aeruginosa CckA
gi 959915700 Pseudomonas syringae CckA
gi 612501466 Neorickettsia sennetsu CckA
gi 499771027 Neorickettsia helminthoeca CckA
gi 778297855 Azospirillum lipoferum CckA
gi 504013803 Azospirillum thiophilum CckA
gi 920579197 Kiloniella spongiae CckA
gi 568206785 Magnetospirillum gryphiswaldense CckA
gi 494150828 Thalassospira xiamenensis CckA
gi 740143786 Thalassospira permensis CckA
gi 126104532 Rhodobacter sphaeroides CckA
gi 915273421 Roseobacter denitrificans CckA
gi 496470349 Silicibacter TrichCH4B CckA
gi 636827499 Brevundimonas naejangsanensis CckA
gi 657606392 Brevundimonas bacteroides CckA
gi Caulobacter crescentus CckA
gi 196477819 Phenylobacterium zucineum CckA H7C7G9
gi 499963148 Maricaulis maris CckA
gi 518803659 Woodsholea maritima CckA
gi 737580073 Hyphomonas atlantica CckA
gi 737623725 Hyphomonas polymorpha CckA
gi 739648268 Sphingomonas jaspsi CckA
gi 948017485 Sphingomonas Leaf30 CckA
gi 739674876 Sphingomonas Ant20 CckA
gi 933871574 Prosthecomicrobium hirschii CckA
gi 490997242 Bartonella henselae CckA
gi 740702495 Bartonella taylorii CckA
gi 640664310 Ochrobactrum intermedium CckA
gi 738679872 Ochrobactrum anthropi CckA
gi 489061410 Brucella WSM3626 CckA
gi 652882861 Mesorhizobium metallidurans CckA
gi 496151501 Mesorhizobium ciceri CckA
gi 503297199 Mesorhizobium ciceri CckA
gi 754557928 Ahrensia kielensis CckA
gi 737099256 Devosia psychrophila CckA
gi 806811338 Agrobacterium tumefaciens CckA
gi 983573890 Pleomorphomonas koreensis CckA
gi 652396579 Pleomorphomonas oryzae CckA
gi 652396820 Pleomorphomonas oryzae CckA
gi 750148216 Labrenzia alexandrii CckA
gi 504703274 Methylocystis SC2 CckA
gi 953943235 Blastochloris viridis CckA
gi 501558063 Oligotropha carboxidovorans CckA
gi 752697953 Nitrobacter winogradskyi CckA
gi 636814770 Bradyrhizobium japonicum CckA
gi 908623163 Rhodopseudomonas palustris CckA
gi 983689510 Bradyrhizobium BR 10303 CckA
gi 951475261 Bradyrhizobium retamae CckA

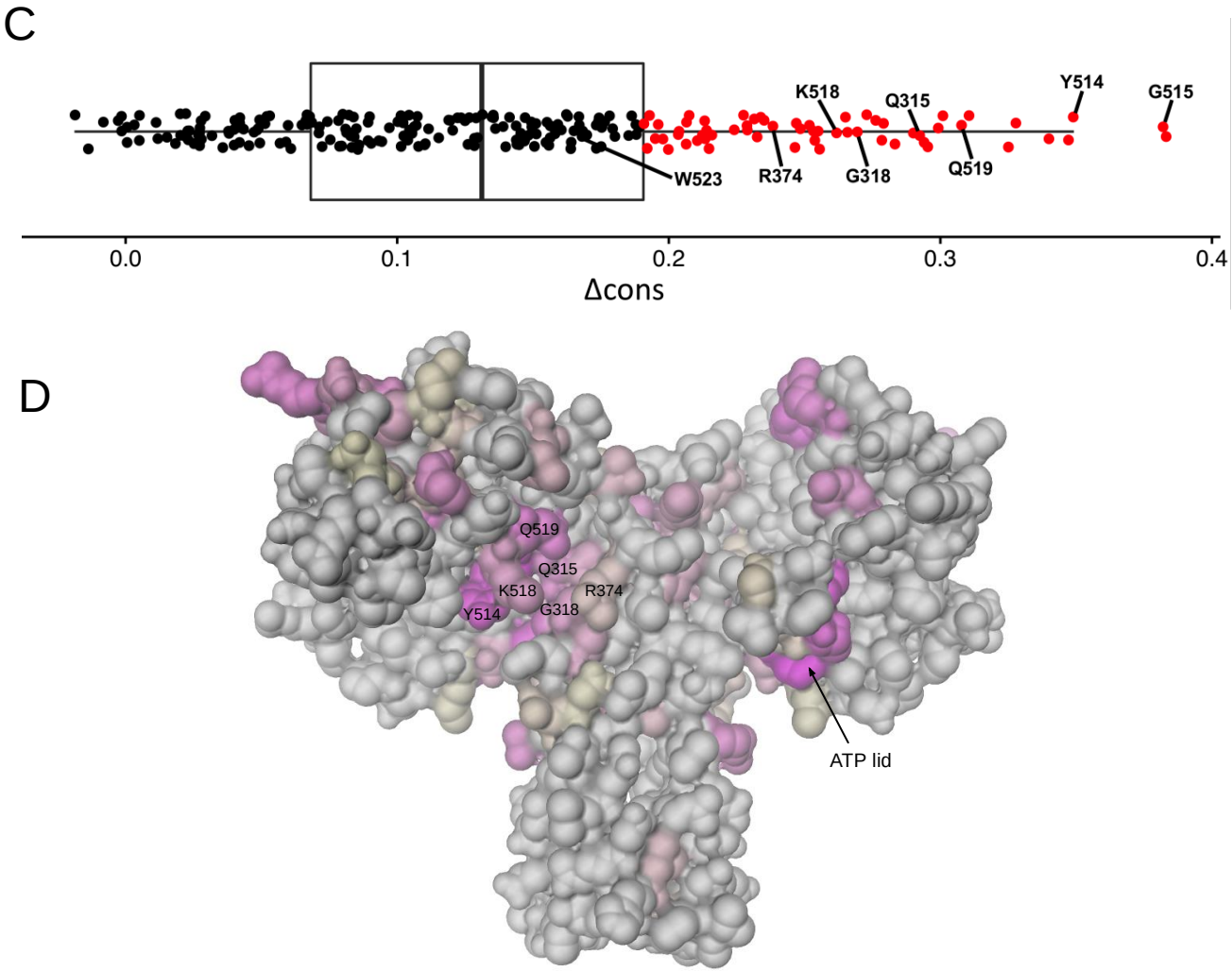

fig. S7. Consensus tree analysis for CckA orthologs and paralogs. (**A**) Bootstrap consensus tree analysis (500 replicates) of CckA orthologs built using the Neighbor-Joining method (*47*). Distances were computed using the Jones-Taylor-Thornton matrix-based method (*48*). The percentage of replicate trees in which the associated taxa clustered together in the bootstrap test (500 replicates) are shown next to the branches (*49*). The rate variation among sites was modeled with a gamma distribution (shape parameter = 1). All ambiguous positions were removed for each sequence pair. Analyses were conducted in MEGA6 (*50*). (B) Combined consensus tree (500 replicates) of CckA orthologs (black) and paralogs (blue). (C) Boxplot of distribution of CckA Δcons scores. Sites scoring in the upper quartile are shown in red. (D) CckA Δcons scores in the upper quartile mapped onto the CckA structure as a color gradient (yellow to magenta, low to high Δcons; view as in Fig. 4A). Residues defining the c-di-GMP binding site at the DHp/CA interface are labeled.

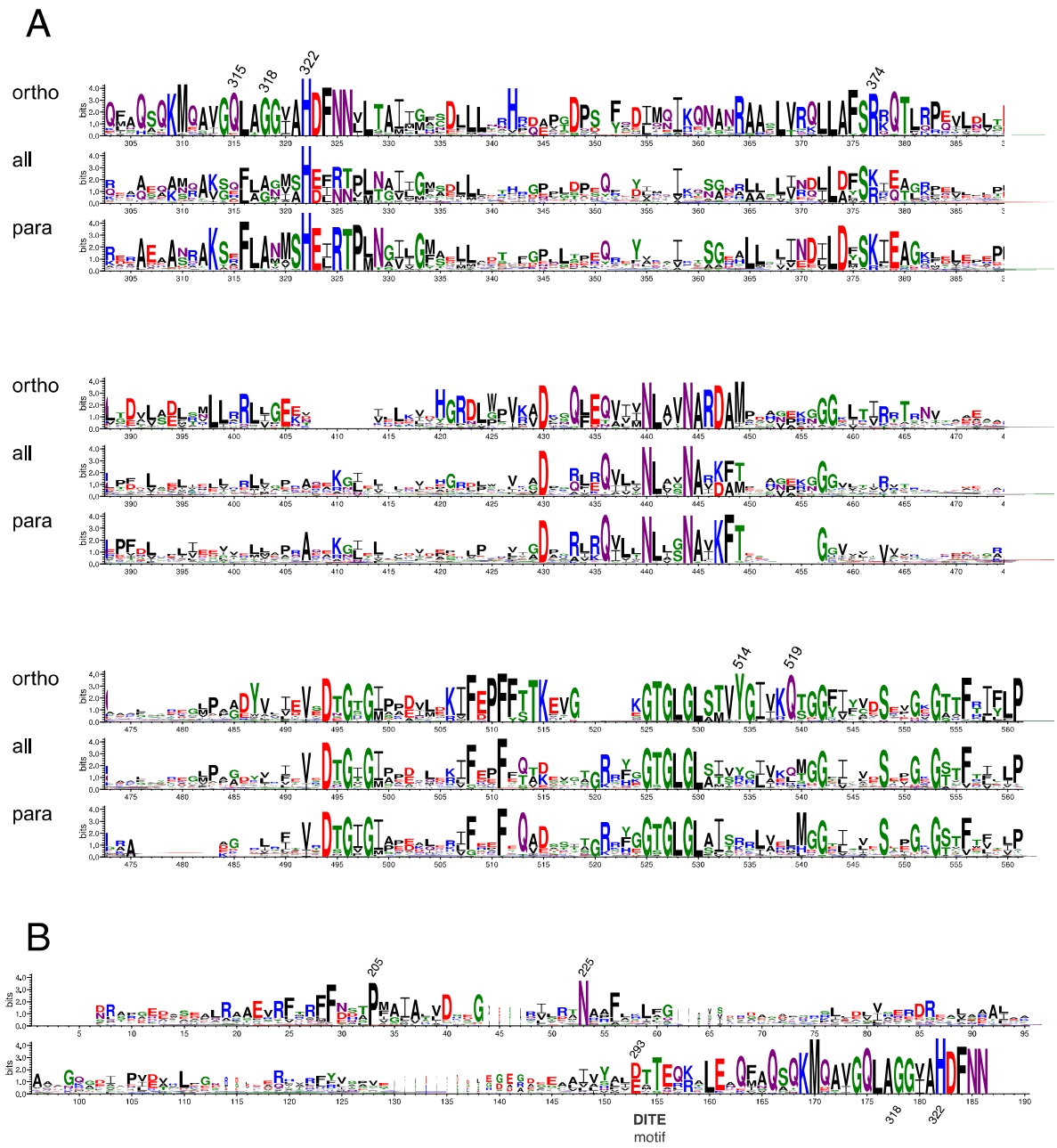

fig. S8. Residue conservation in CckA orthologs and paralogs. (**A**) Sequence logos (*51*) are shown based on 49 sequences of CckA orthologs (top), 75 sequences of paralogs (bottom) and for both groups together (middle). Latter graph highlights the residues that are essential for general histidine kinase function. See also fig. S7B. Residues specifically conserved (SDPs) in the orthologous CckA group (top) are labeled with their CckA number, otherwise global residue numbering. (**B**) N-terminal extension of the ortho-group logo towards the proximal PAS domain region, using only the 36 sequences that could be aligned confidently. Note that this region is very variable with the exception of a conserved P and N, and the DITE motif (labeled with CckA residue numbers).